Electronic Supplementary Material (ESI) for New Journal of Chemistry.

Supporting Information

Sulfonated Graphene Supported Nano Copper MoS_2 Network for Non-enzymatic Simultaneous Sensing of Dopamine and Serotonin

Baishali Mahanta[a], *Hasan Al Mamun*[b], *Rana Sanjay Kumar Singh*[b] *and Lakhya Jyoti Borthakur*[b*]

[a]*Department of Chemistry, Gauhati University, Guwahati-781014, India.*

[b]*Department of Chemistry, Nowgong College (Autonomous), Assam-78200, India.*

E-mail: lborthakurpub2022@gmail.com

S1 Experimental

S1.1 Chemicals and Reagents

Dopamine hydrochloride, Serotonin hydrochloride, and Sodium molybdate were purchased from Sigma Aldrich (99.0% purity). Copper acetate (99.8%) pure was purchased from Merck. Graphite powder (99.8%), Orthophosphoric acid (H_3PO_4, 85%), Thiourea, Potassium dihydro phosphate, Potassium hydrogen phosphate, Potassium permanganate, Sulphuric acid, Hydrogen peroxide, and Sodium Hydroxide used were analytical grade. DW was used in all the experiments.

S1.2 Preparation.

The schematic reactions for the synthesize of *MoS_2/SG/Cu* nanocomposite are given in *Scheme S1* as follows:

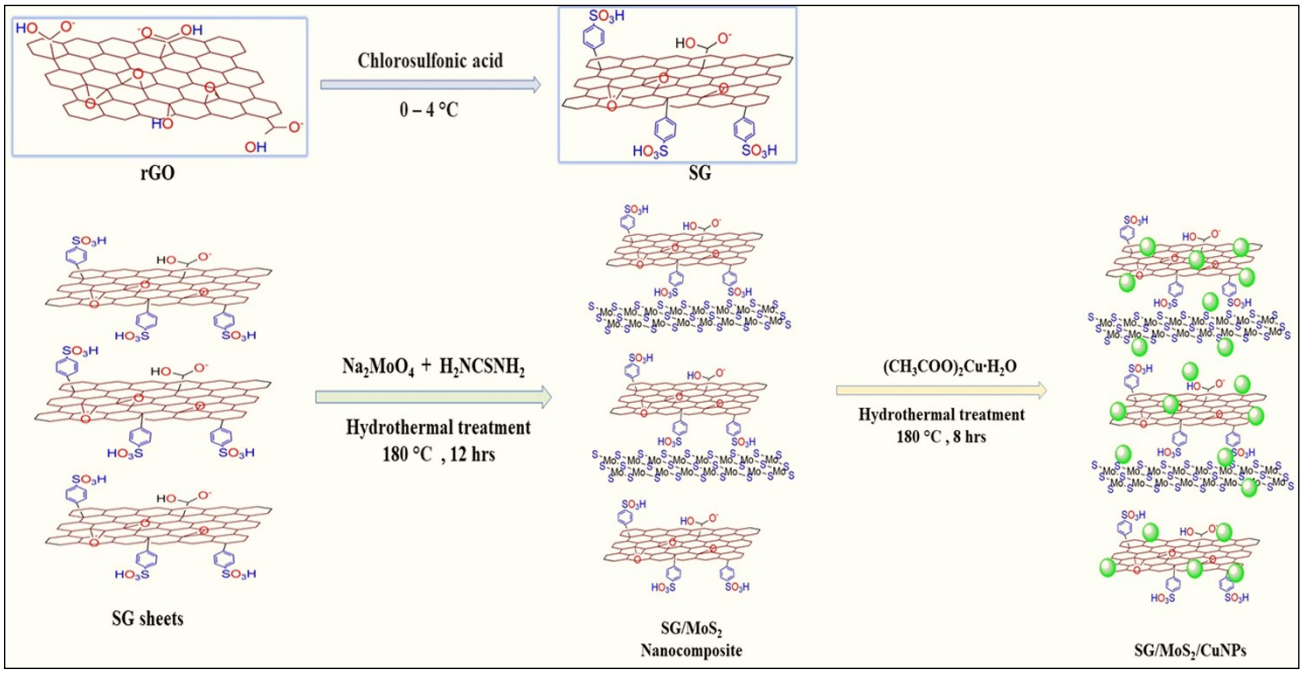

Scheme S1: Scheme representing the synthesis of MoS_2/SG/Cu nanocomposite

S1.3 Instrumentation and Apparatus

X-ray diffraction (XRD) patterns were obtained using the Bruker D8 Discover with Cu-Kα radiation ((λ = 1.54056 Å) with a 2θ range of 10 ° to 80 °. The Raman spectra were obtained on a Dongwoo Optron (Model: Vector-01FX) confocal Raman spectrometer using an argon-ion (488 nm) laser source. Scanning electron microscopy (SEM) was performed using a JEOL (JSM-

7000F) instrument equipped with energy-dispersive X-ray spectroscopy (EDAX) for morphological characterization and semi-quantitative information from the sample surface at a step size of 0.01 ° for the crystal structure analysis. Transmission electron microscope (TEM) observations were carried out using a JEOL 200 kV transmission electron microscope. X-ray photoelectron spectroscopy (XPS) analysis was carried out on a PHI 5000 Versa Probe III X-ray photoelectron spectrometer. The electrochemical activities of the modified electrodes were studied by Cyclic Voltammetry (CV), Chronoamperometry, EIS in a three-electrode system with a platinum wire, Ag/AgCl and a modified GCE as the auxiliary, reference, and the working electrode respectively. All the electrochemical experiments were performed in 0.1 M Phosphate Buffer Solution (PBS).

S1.4 Electrode preparation

For each experiment, the GCE (Glassy carbon electrode) (working electrode) surface was polished in Al_2O_3 slurries (1 μM and 0.05 μM) followed by repetitive ultrasonic washing with DIW-EtOH mixture until a mirror-clean surface was obtained. The working electrode was fabricated by drop-casting MoS_2/SG/Cu nanocomposite over the polished GCE. The nanocomposite was dispersed in a 2:1 isopropanol: Nafion mixture under ultrasonication till a uniform texture was achieved, where Nafion acts as the binder. A similar procedure was repeated to fabricate SG/MoS_2 modified GCE. The electrodes obtained were dried at R.T. and used for further electrochemical sensing.

S2 Schematic representation of reactions:

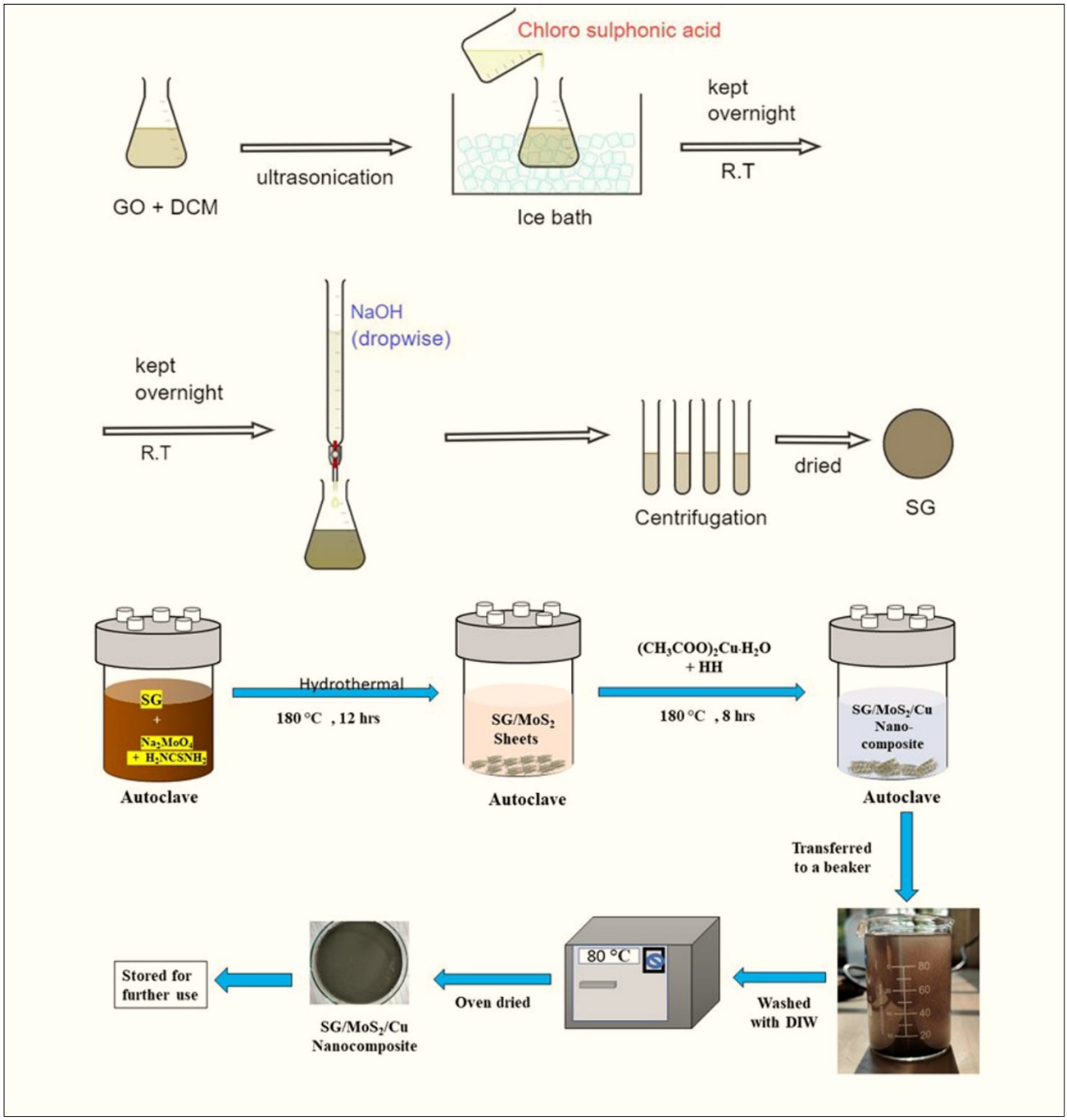

Scheme S2: Schematic pictorial representation of preparation of MoS_2/SG/CuNP electrocatalyst

S3 Results and Discussions

S3.1 Raman Analysis

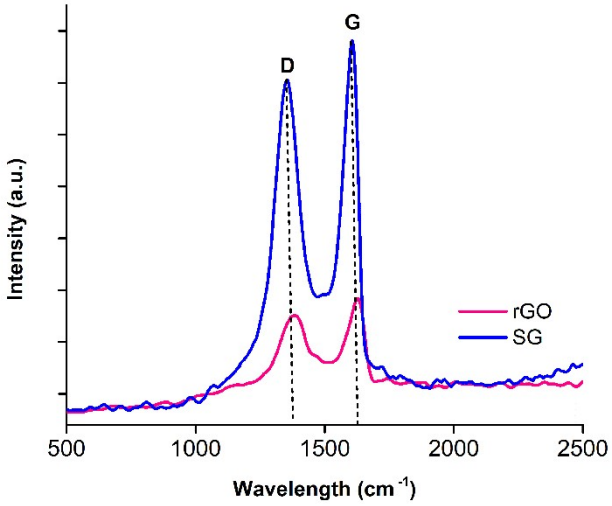

Figure S3: Raman spectra of rGO and SG

S3.2 SEM Analysis

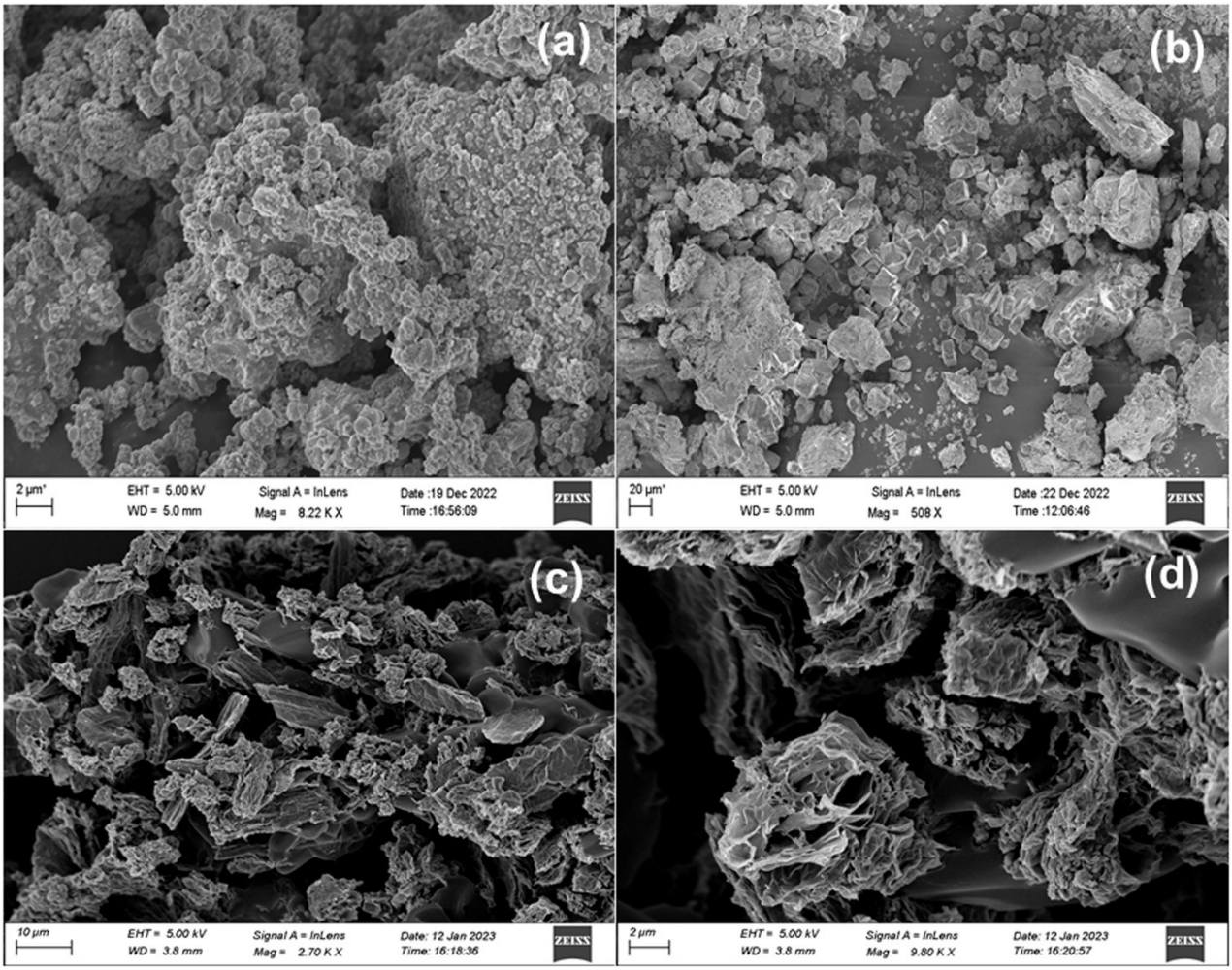

Figure S4 A: SEM imaging of (a) – (b) of Copper nanoparticles; (c) – (d) SG

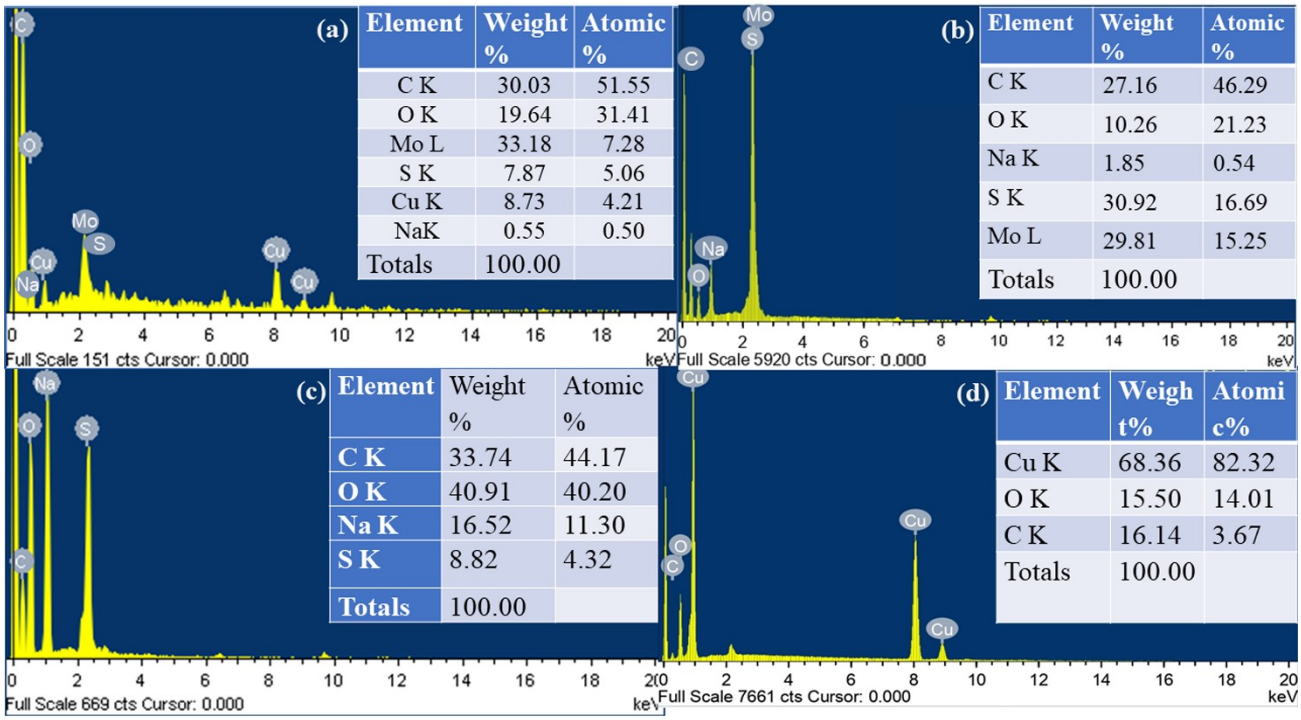

Figure S4 B: EDX of (a) MoS_2/SG/CuNP (b) MoS_2/SG (c) SG and (d) CuNP

S4 Electrochemical behaviour of MoS_2/SG/CuNP/GCE for the determination of DA and 5-HT individually

S4.1 Effect of Change in pH

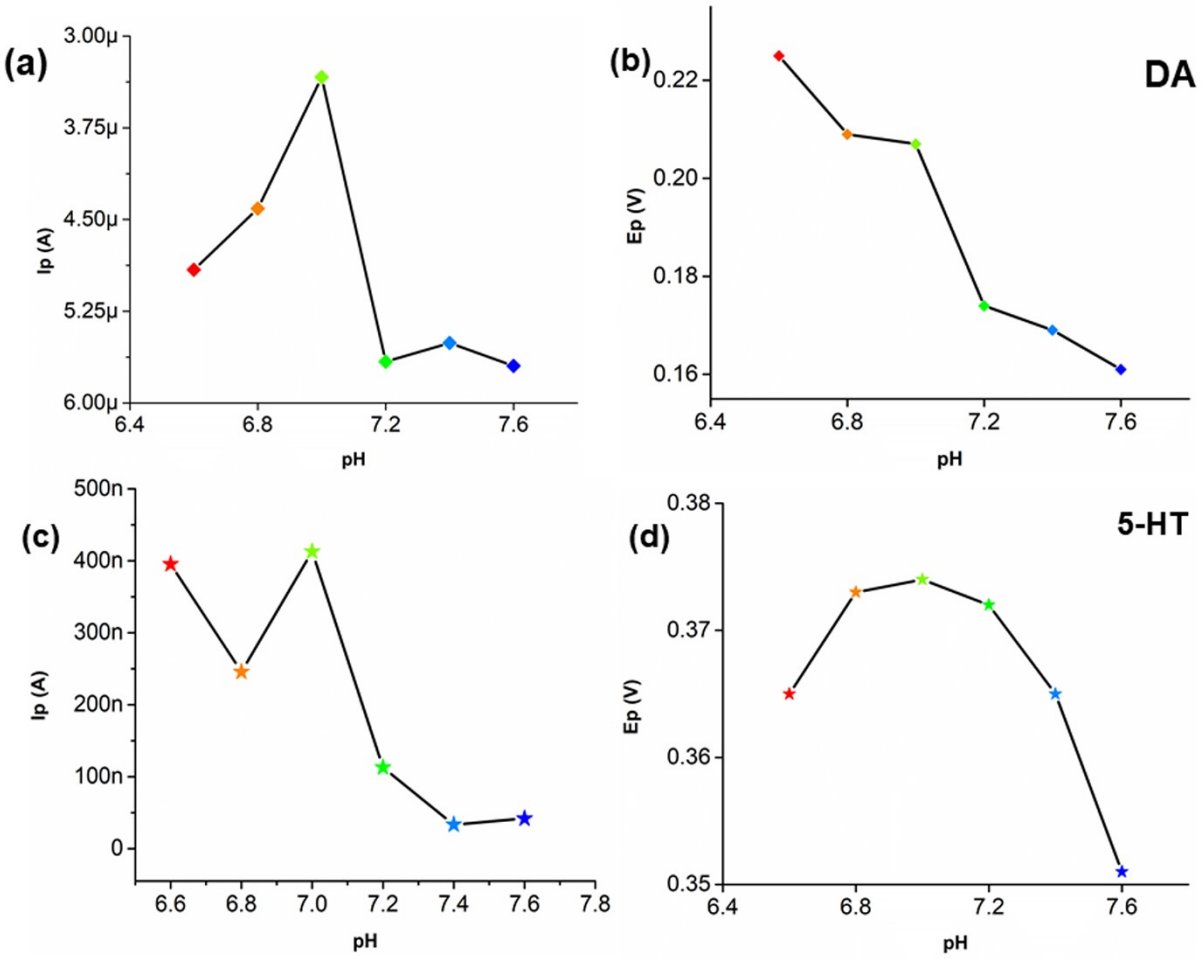

Figure S5: (a), (d) LAC for Ip vs pH; and (b), (d) for Ep vs pH, at 0.1M PBS for MoS_2/SG/CuNP/GCE

S4.2 Effect of Scan rate

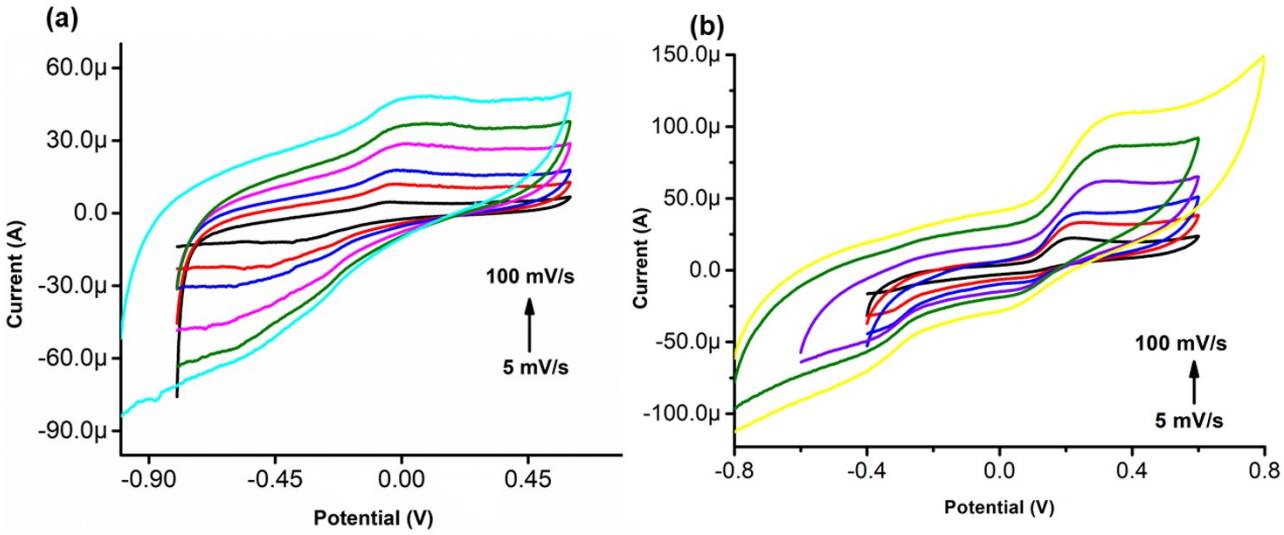

Figure S6: Effect of varying scan rate from 5mV/s to 100mV/s (a) DA and (b) 5-HT, at 0.1M PBS for MoS_2/SG/CuNP/GCE

S4.3 Table S1: Comparison of LOD of different electrodes

Electrode		Linear Electrode (μM)	Detection Limit (nM)	Technique	Reference
ZrO_2-CuO co-doped	DA	0.008 - 7.2	3.09	DPV	[1]
CeO_2 Carbon paste electrode	5-HT	0.008 - 7.9	3.42		
Rotating Disc electrode	DA	0.01- 2	< 2.01	SWV	[2]
	5-HT	0.01- 2	2.01		
GO/PANI/AuNP	5-HT	0.2 -10	11.7	DPV	[3]
CNF electrode	DA	-	50	DPV	[4]
CNF electrode	5-HT	-	250	DPV	[5]
Nafion and Multiwall Carbon Nanotube Modified Ultra nano crystalline Diamond Microelectrodes	DA	0.18 -1.7	5.4		
MoS_2/SG/CuNP	5-HT	0.0005 - 0.005	0.62	CV	[*Our Work*]
	DA	0.001 - 0.05	0.85		

S4.4 Repeatability, Stability, and Interference studies.

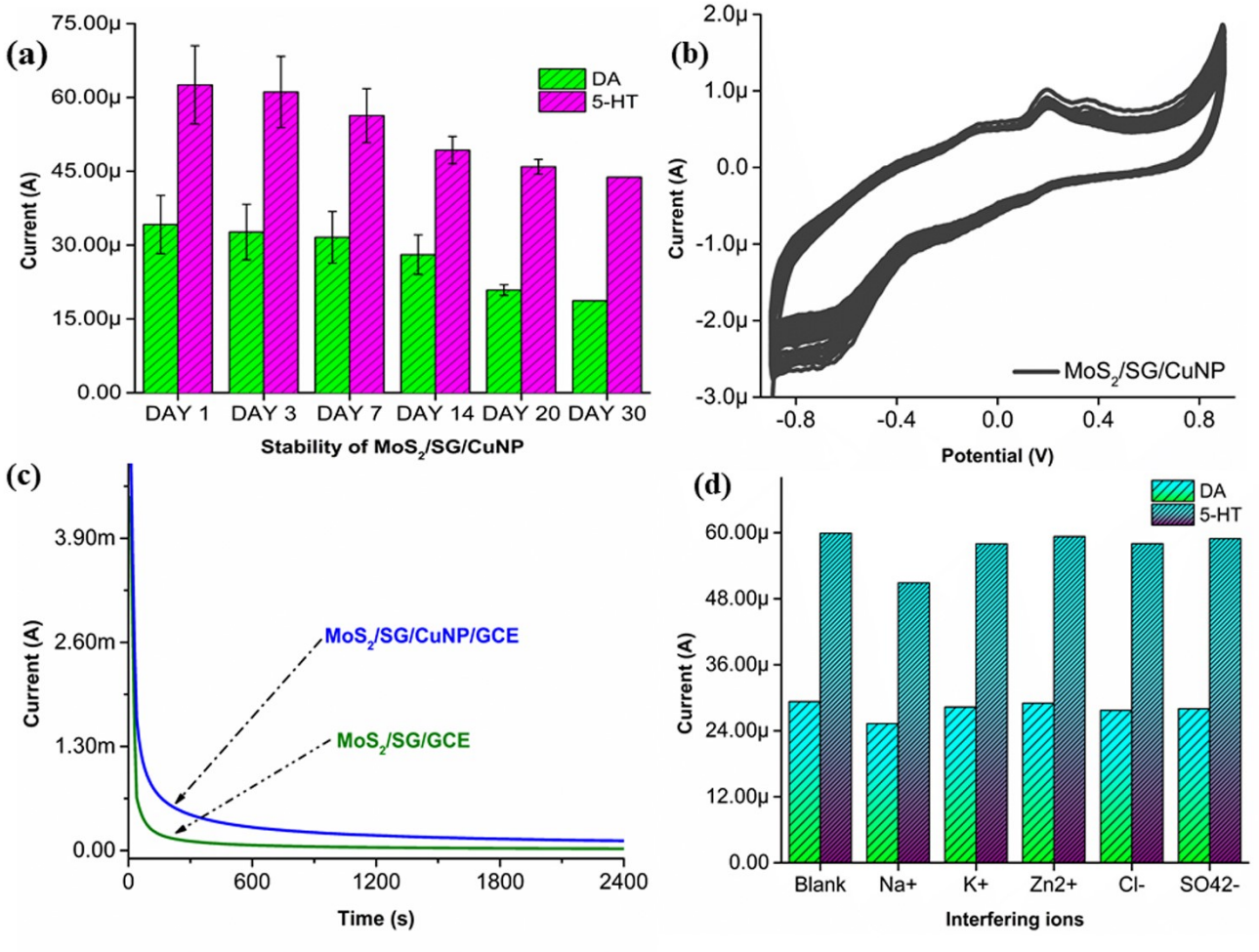

Figure S7: (a) Stability over a period of 30 days (b) Cyclic stability for 600 sweep cycles (c) Chronoamperometric stability comparison with SG/MoS_2/SG/GCE; (d) Anti-interfering capacity of SG/CuNP modified electrode

S4.5 Table S2: The recovery rate of DA and 5-HT in human urine samples using MoS_2/SG/CuNP /GCE as the working electrode

Urine Sample	Analyte	Spiked (µM)	Found (µM)	Recovery (%)
Sample 1	DA	40	37.5	93.80
	5-HT	40	37.3	93.31
Sample 2	DA	30	28.2	94.12
	5-HT	30	28.7	95.94
Sample 3	DA	20	19.5	97.82
	5-HT	20	19.3	96.76
Sample 4	DA	10	9.7	96.69
	5-HT	10	9.8	98.03
Sample 5	DA	1	1.05	105.21
	5-HT	1	.98	98.10
Sample 6	DA	0.1	0.09	97.80
	5-HT	0.1	0.1	101.1
Sample 7	DA	0.01	0.009	97.81
	5-HT	0.01	0.009	98.03

S.5 Representation of Error Bars.

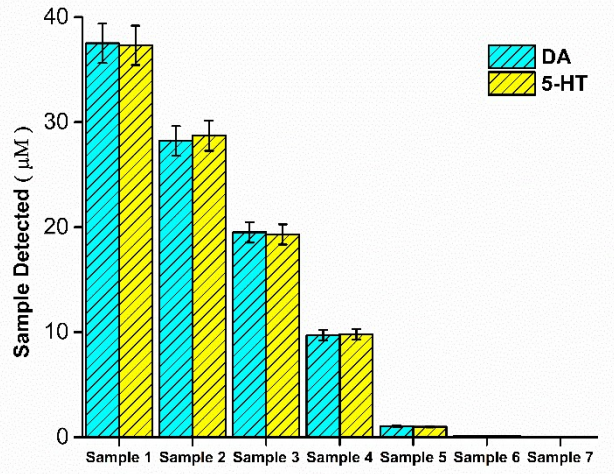

Figure S8: Representation of standard recovery of samples indicating the error bars

S.6 Validation of the recoveries by classical detection technique

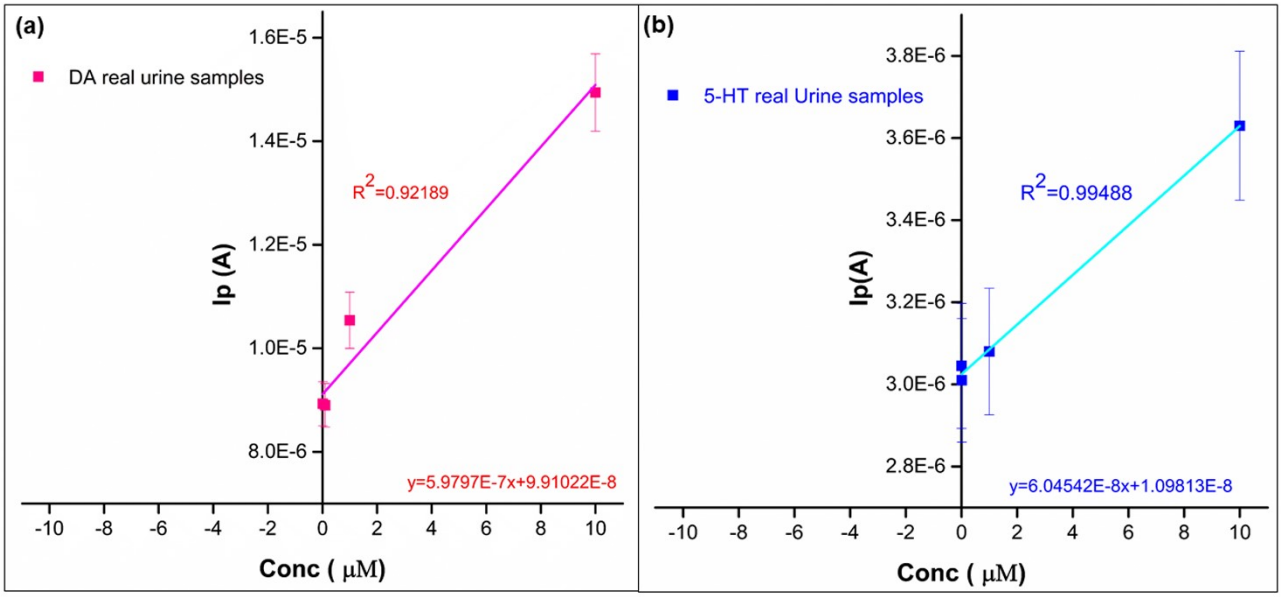

Figure S9: Linear dependence on anodic peaks at spiked lower concentration from 10 – 0.01 μM for analytes (a) DA and (b) 5-HT in real human urine samples

References:

1. F. Fariba and M. B. Gholivand, *Talanta*, 2022, **239**, 122982. DOI: 10.1016/j.talanta.2021.122982

2. M. Kundys-Siedlecka, E. Bączyńska, & M. Jönsson-Niedziółka, *Anal. chem.*, 2019, **91**, 10908-10913. https://doi.org/10.1021/acs.analchem.9b02967

3. K. Mahato, B. Purohit, K. Bhardwaj, A. Jaiswal, P. Chandra, *Biosens. Bioelectron.*, 2019, **142**, 111502. DOI: 10.1016/j.bios.2019.111502

4. E. Rand, A. Periyakaruppan, Z Tanaka, A. D. Zhang, M. P. Marsh, R. J. Andrews, K. H. Lee, B. Chen, M. Meyyappan, J. E. Koehne, *Biosen.Bioelectron.*, 2013, **42**, 434-438. DOI: 10.1016/j.bios.2012.10.080

5. A. Y. Chang, S. Siddiqui, & P. U. Arumugam, *Micromachines*, 2021, **12**, 523. DOI: 10.3390/mi12050523